ISSN: 2664-9640

Design of lithium-ion battery balancing circuit for electric vehicles

Jing Wu, Bo Zhang, Meng Huang, Xuan Zhang, Chaolong Zhang, Shanhe Jiang

School of Electronic Engineering and Intelligent Manufacturing, Anqing Normal University
Anqing 24601, China

Abstract

A novel balancing circuit is designed in the paper to solve the inconsistency problem of lithium-ion batteries in the battery packs of new energy vehicles. Firstly, terminal voltage of every battery in the pack measured. Then, an extended Kalman filter (EKF) algorithm is used to transform the battery voltage to battery SOC with high accuracy. Then, a novel balancing circuit is designed based on estimated battery SOC and battery balancing method. In the experiment, the maximum absolute error and mean absolute error are respectively 0.0184 and 0.0035 when initial battery SOC is decided, and the maximum absolute error and mean absolute error are respectively 0.5 and 0.0038 otherwise. Meanwhile, the SOC difference of batteries reduces from 7% to 1.2% in 133 s, which the designed balancing circuit has fast balancing speed and perfect performance.

Keywords

Lithium-ion batteries, balancing circuit, SOC, EKF algorithm.

1. Introduction

Power battery system is the main device for energy storage of electric vehicles[1,2]. The system is composed of many lithium-ions which are series-parallel connection. Initial difference and usage difference exist in various batteries which leads to the different parameters on battery voltage, capacity ,internal resistance and so on. With the constant discharging and charging on battery, the inconsistency gradually gets worse[3-5].The performance of battery is attenuated, which leads to thermal runaway. The inconsistency is reduced and the safety is raised by balancing circuit of power battery[6-10].

The balancing methods of power battery are divided into the passive balancing method and the active balancing method according to the way of energy transfer[11-16]. Passive balancing method is energy dissipated balancing. The excess electric quantities are transformed to thermal energy by resistor. This method consumes high voltage battery and high power battery. But the disadvantages are that the redundant energy cannot be transformed to the low capacity battery.

Active balancing method is non-dissipated balancing which achieves energy transfer among various batteries by topological structure and control strategy of the circuit . Active balancing methods are divided into transformer blancing, inductance balancing and capacitance balancing, but it is difficult to develop topology about small size, easy integration, low cost, high balancing speed and high reliability.

According to the difference of control variables, the methods of battery balancing are divided into voltage balance, state of charge(SOC)balance and so on. Voltage balance measures the voltage of the battery for balancing[17-19]. The disadvantages are that the real power status inside the battery cannot be reflected and the balancing is non-ideal. The SOC effectively represents the internal battery state, but the disadvantage is that the SOC cannot be measured

ISSN: 2664-9640

directly. The battery SOC need be calculated by effective method. The estimation accuracy of SOC directly depends on the designed SOC derivation method[20,21] .

The main SOC estimation methods include open-circuit voltage method, ampere-hour integration method, neural network , Kalman filter algorithm and so on. Open circuit voltage method needs preserve the battery for a long time. Thus, the open circuit voltage of the battery can be measured accurately[22,23] . Ampere-hour integration method depends on initial battery SOC value. If the initial value is inaccurate , the error is larger. Neural network needs to use a large number of historical experimental data . The computation is large and the hardware requirement is high. Extended Kalman Filter (EKF) is an extension of standard Kalman filter in nonlinear case[24,25]. The method uses Taylor series to linearize a nonlinear system. The unique advantage is filtered by Kalman filter for the measured signal in SOC estimation.

In this work, an active balancing circuit based on SOC and the battery pack is designed which can reduce the battery inconsistency to improve security and prolong the remaining useful life of battery. At first, the terminal voltage of each battery is measured . Then the battery voltage is converted to SOC measured by EKF algorithm. After that, active balancing circuit of battery pack based on battery balancing is designed. The advantages are that the balancing time is short and the balancing current is large during the testing process.

2. Theoretical Basis

2.1. Establishment of battery model

Owing to the fact that various complex electrochemical reations are conducted inside the battery when charging, the accurate battery model is difficult to establish. The current commonly used battery models include mathematical model, electrochemical model, coupling model, neural network and equivalent circuit model. As shown in Fig.1 , the second-order RC equivalent circuit model is an accurate battery model .The model is applied in this work.

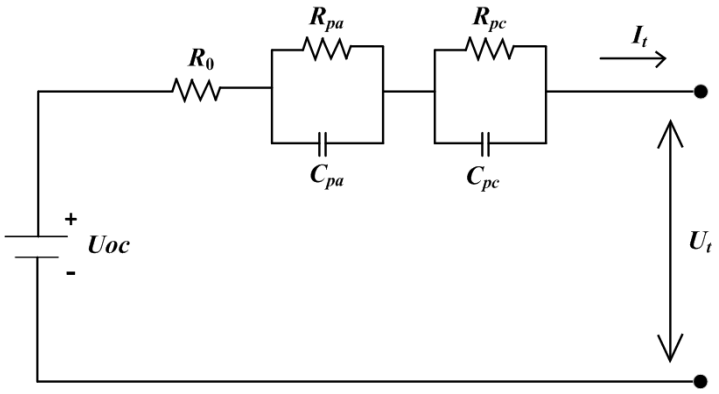

Fig.1 Second-order RC equivalent circuit model

Assume U_{OC} is the open circuit voltage of the battery; R_0 is the internal resistance; Rpa, Cpa are the polarization resistance and polarization capacitance, respectively; Rpc, Cpc are the concentration resistance and the concentration capacitance, respectively. The equations of the circuit model are defined as following

$$\dot{U}_1 = \frac{I}{C_{pa}} - \frac{U_1}{R_{pa} \cdot C_{pa}} \quad , \tag{1}$$

$$\dot{U}_2 = \frac{I}{C_{pc}} - \frac{U_2}{R_{pc} \cdot C_{pc}} \quad , \tag{2}$$

$$U = U_{OC} - U_1 - U_2 - I \cdot R_0 \quad , \tag{3}$$

ISSN: 2664-9640

2.2. Power battery

1)Parameter identification of ohmic internal resistance

The 2.4 Ah rated capacity of 18650 battery is adopted in the HPPC test.

The discharging data are collected in the HPPC test. The detailed process is as following. Batteries are discharged by 1 C current constanly for 6 minutes at 25 ℃ . Then the batteries are preserved for 1 hour, which is showed in Fig.2. The steps are repeated ten times until the battery SOC drops to 0, which is showed in Fig.3. Meanwhile, the test is finished. In Fig.2, the static state is before time C. Time C and time E are the starting and ending moment, respectively. From time E to time G is also a static stage. From Fig.2 , voltage drops before time C and increases at time E when the battery begin to discharge. Because of the characteristics of RC network , a short voltage pulse is impossible. The internal resistance can be obtained according to :

$$R_0 = \frac{(U_C - U_D) + (U_F - U_E)}{2I} \tag{4}$$

where U_C,U_D,U_E,U_F are the voltage of time C,time D, time E,time F, respectively.

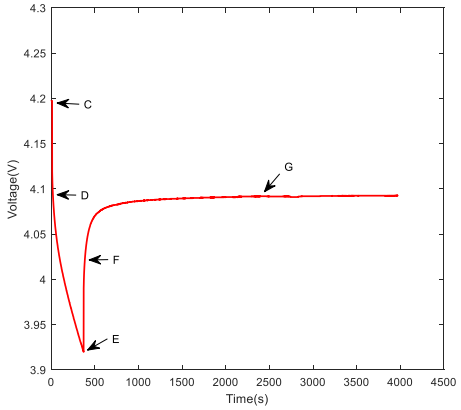

Fig.2 Battery discharge voltage curve in a pulse of HPPC test

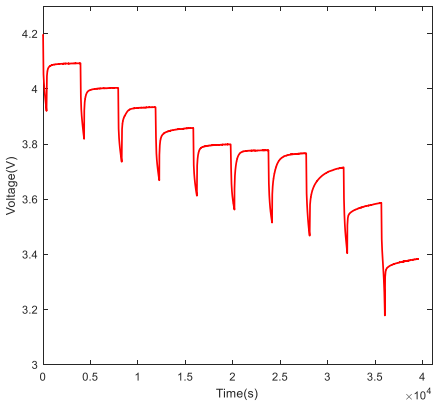

Fig.3 Battery discharge voltage curve in the HPPC test

The battery is preserved for a long time before HPPC test. The polarization characteristic and diffusion effect are dynamic characteristic of battery. Time constant is obtained from Equs.(1)-(2):

$$\tau(\mathrm{s}) = \mathrm{R}(\mathrm{M}\Omega) \cdot \mathrm{C}(\mathrm{uF}) \tag{5}$$

$$U_1(t) = U_1(0)e^{-\frac{t}{\tau_1}} + IR_{pa}(1 - e^{-\frac{t}{\tau_1}}) \tag{6}$$

$$U_2(t) = U_2(0)e^{-\frac{t}{\tau_2}} + IR_{pc}(1 - e^{-\frac{t}{\tau_2}}) \tag{7}$$

ISSN: 2664-9640

Where,$U_1(0)$,$U_2(0)$ are the initial voltage of the two RC network, respectively; τ_1 is the polarization time constant; τ_2 is the concentration time constant; t is the response time of the battery polarization effect.

After the discharge, the battery preserved voltage response curve is from time E to time G. Therefore, it can be considered as the zero-input response of RC network. The terminal voltage expression can be obtained as following

$$\mathrm{U}(t) = U_{OC} - U_1(0)e^{-\frac{t}{\tau_1}} - U_2(0)e^{-\frac{t}{\tau_2}} \tag{8}$$

After preserving a long time, the difference value between U_{OC} and the voltage after time F. Using the Curve Fitting of Matlab, the exponential fitting of polarization is as following

$$f(\mathrm{t}) = \mathrm{a}e^{-\lambda_1 t} + \mathrm{b}e^{-\lambda_2 t} \tag{9}$$

Referencing Equs. (8) and (9),Equ.(10) is obtained.

$$\mathrm{a} = U_1(0)\,, b = U_2(0)\,, \tau_1 = {}^{1}/_{\lambda_1}\,, \tau_1 = {}^{1}/_{\lambda_2} \tag{10}$$

The battery has been preserved a long time before time D. The polarization effect can be considered as 0. According to $U_1(0) = U_2(0) = 0$, it can be considered as the zero-state response of RC network. Referencing Eqs.(6)and (7),Eqs.(11) and (12) can be obtained as following

$$U_1(t) = IR_{pa}(1 - e^{-\frac{t}{\tau_1}}) \tag{11}$$

$$U_2(t) = IR_{pc}(1 - e^{-\frac{t}{\tau_2}}) \tag{12}$$

It can be considered as 0 owing to the fact that the changing time from E to F is short. The polarization volatge is almost constant. Referencing Eqs.(11)and(12),Eqs.(13) and (14) can obtained as following

$$U_1(0) = IR_{pa} \tag{13}$$

$$U_2(0) = IR_{pc} \tag{14}$$

Considering Eqs. (5), (10), (13) and (14), the model parameters can be obtained. The result is as follows

$$\begin{aligned} \mathrm{R0} &= 0.03249\ \Omega \\ \mathrm{Rpa} &= 0.0084\ \Omega \\ \mathrm{Rpc} &= 0.02952\ \Omega \\ \mathrm{Cpa} &= 69937.4\ \mathrm{nF} \\ \mathrm{Cpc} &= 1710.64\ \mathrm{nF} \end{aligned} \tag{15}$$

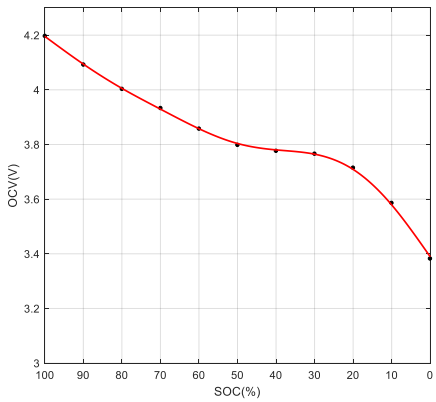

Fig. 4 Fitting curve of OCV and SOC

The relationship of U_{OCV} and SOC is showed in Fig .4, which is calculated by using the curve fitting tool as following

ISSN: 2664-9640

$$U_{OCV} = -165.2724\times SOC^{8}+622.6588 \times SOC^{7}-922.4608 \times SOC^{6}+673.6454 \times SOC^{5}-248.9618 \times SOC^{4}+46.5634 \times SOC^{3}-7.9146\times SOC^{2}+2.5581 \times SOC +3.3812 \quad (16)$$

2.3. SOC estimation of battery based on EKF algorithm

After establishing the battery's second-order RC equivalent circuit model, its parameters are computed. Then, EKF algorithm is used to estimate the battery SOC. The initial battery SOC is decided or not. Therefore, two different tests are performed. The test 1 denotes the decided initial battery SOC and the test 2 is the opposite.

Firstly, the EKF algorithm is applied to estimate battery SOC on the basis of the measured battery voltage in the test 1, and the results are revealed in Fig.5. Meanwhile, estimation error is calculated in Fig.6. Its maximum absolute error and mean absolute error are 0.0184 and 0.0035, respectively.

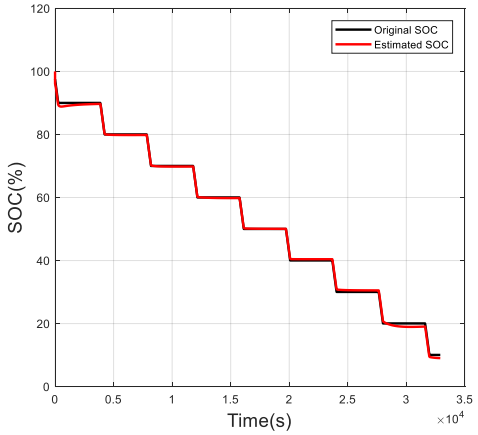

Fig.5 The estimation results in test 1

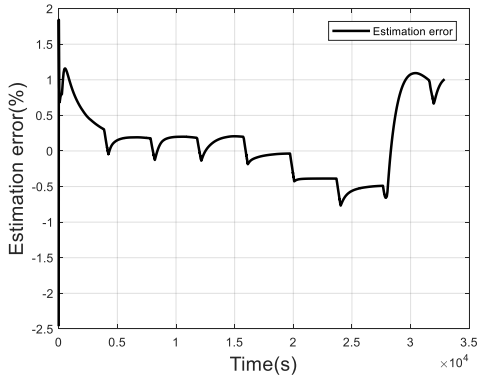

Fig. 6 The estimation error in test 1

In the test 2, the initial battery SOC is set to 0.5 for its undetermined value. Fig.7 shows the estimation results. The estimated battery SOC value converges to the true value even if the original SOC differs completely. Fig.8 demonstrates the estimation error. Its maximum absolute error and mean absolute error are 0.5 and 0.0038, respectively.

ISSN: 2664-9640

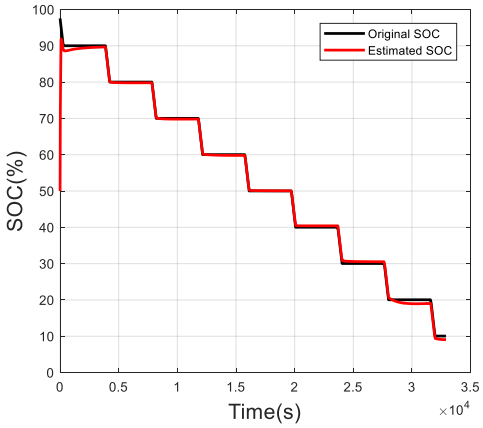

Fig. 7 The estimation results in test 2

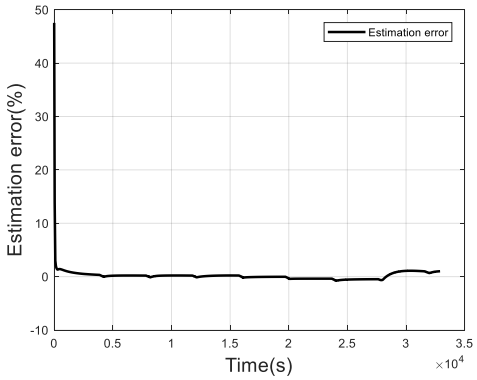

Fig. 8 The estimation error in test 2

As can be seen from Fig.5 to Fig. 8, when the initial value of the battery SOC is uncertain, the estimated SOCs can both quickly converge to the original SOCs, and this indicates that the EKF algorithm has the advantages of high accuracy, fast convergence speed and strong practicability in the estimation of the battery SOC. The method is applied to battery balancing to improve balancing efficiency.

2.4. Simulation design on active balancing circuit of battery pack

The active balancing circuit designed in this work is shown in Fig.9.The PWM signal is used to control the switch S, and the battery B1 charges the external battery B through the energy storage inductor L. When the switch S is in the on-state, the balancing current i_1 of battery B flows through the loop ① to charge inductor L , and the inductor L stores electric energy in the process. Then the switch is disconnected. The electric energy stored in the inductance L discharges to the external battery B through the loop ②, while the battery B is charging. The balancing circuit is an up and down voltage chopper circuit. Balancing current i_1 can be adjusted by setting different PWM wave duty ratio of switch tube S.

The battery balancing system designed in this work is built through the Simulink module of Matlab. The designed active balancing circuit is shown in Fig.10. Battery 1,Battery2, ..., and Battery 8 are shown in Fig.10. The nominal voltage and rated capacity are set to 3.6 V and 2.4 Ah, respectively. Before balancing, the initial SOCs of batteries are respectively set to 50%, 51%, 52%, 53%, 54%, 55%, 56%, 57%.Charging current is 2.4 A ,the switching frequency is 1 kHz and the duty ratio is 40%.

The range method is adopted in this work, and the process is as following. When the range of the maximum and minimum SOC value exceeds 0.02, the balancing circuit is started. Otherwise it is not started. The program is preformed by the Matlab-function module. The inputs include

ISSN: 2664-9640

the SOC of each battery, the range between the maximum and minimum SOC of each battery and the maximum SOC of the battery. The output of the Matlab-Function module is the input of the If-Action module. It is determined by the set judgment conditions whether the balancing circuit is turned on.

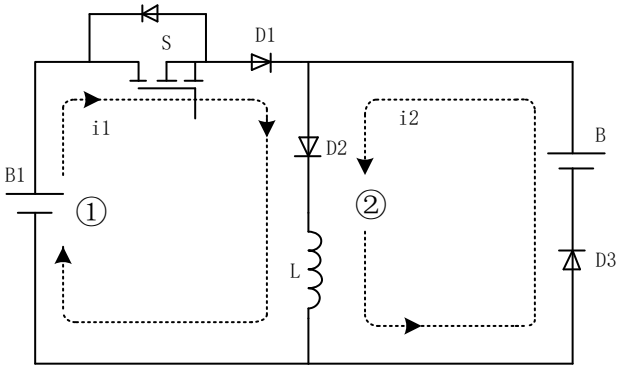

Fig.9 Change balancing equivalent circuit

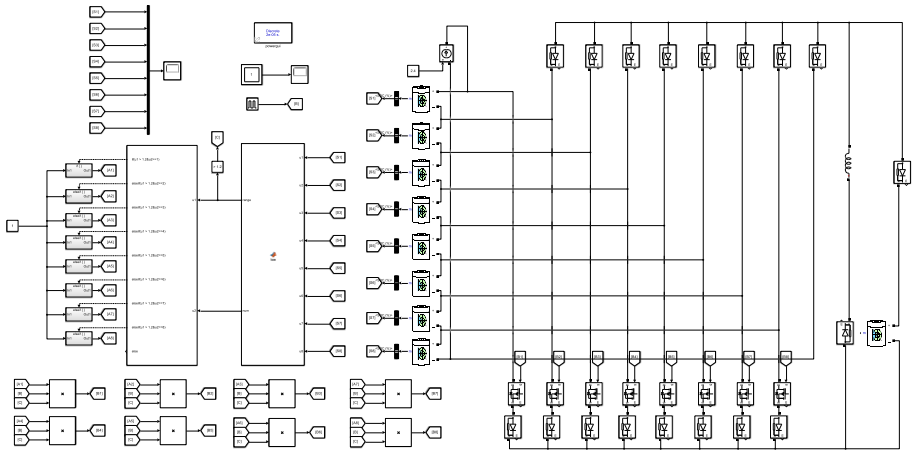

Fig. 10 Active balancing simulation circuit

The charging process of the eight batteries used in the simulation experiment of active balancing is shown in Fig.11. When the simulation is carried out at 133 s, the difference of each battery SOC is basically eliminated and the consistency is formed. The balancing ending condition is met.

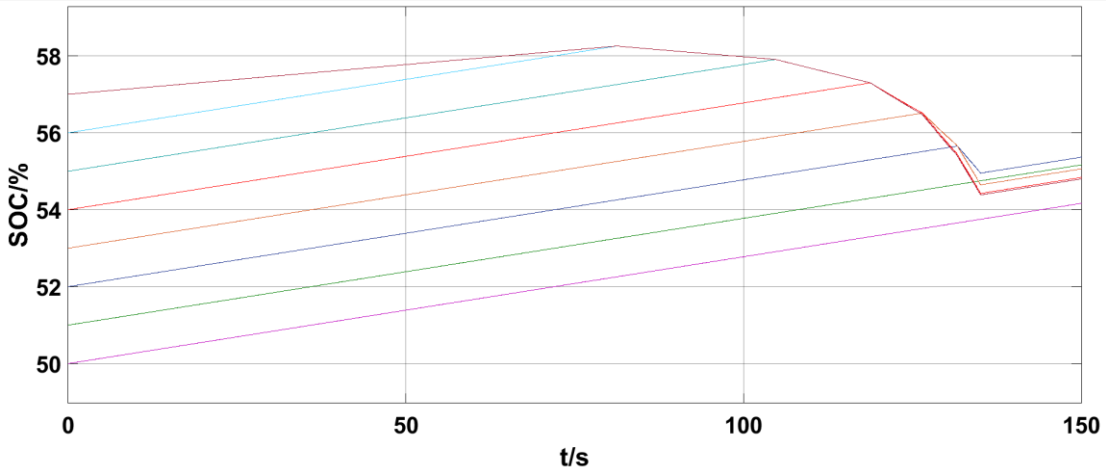

Fig.11 Charge balancing of eight battery SOC

ISSN: 2664-9640

The change of inductance current with time is shown in Fig.12. When the balancing current drops to 0, the active balancing process is ended. The difference of each battery SOC is basically eliminated, and the consistency is formed.

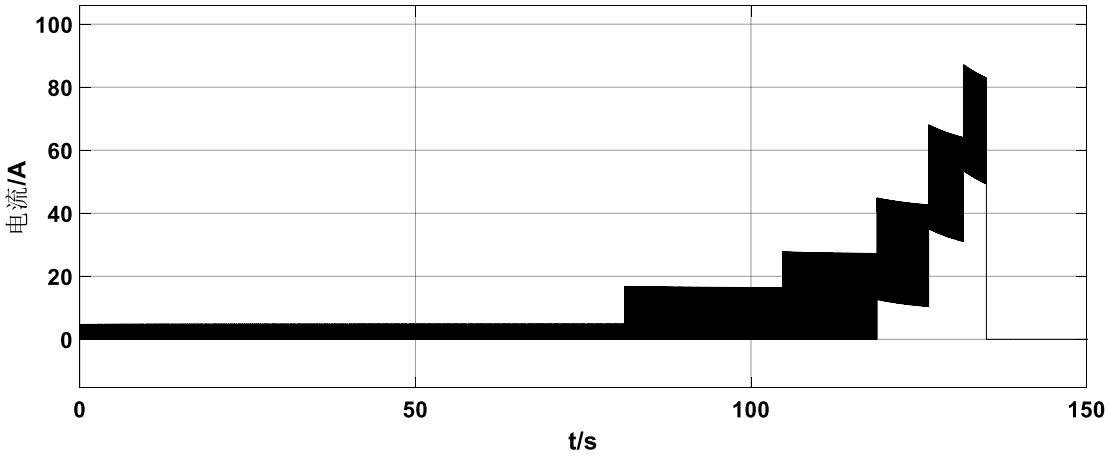

Fig.12 The inductor current of charge balancing circuit

Steady-state inductance current of each stage is shown in Fig.13.

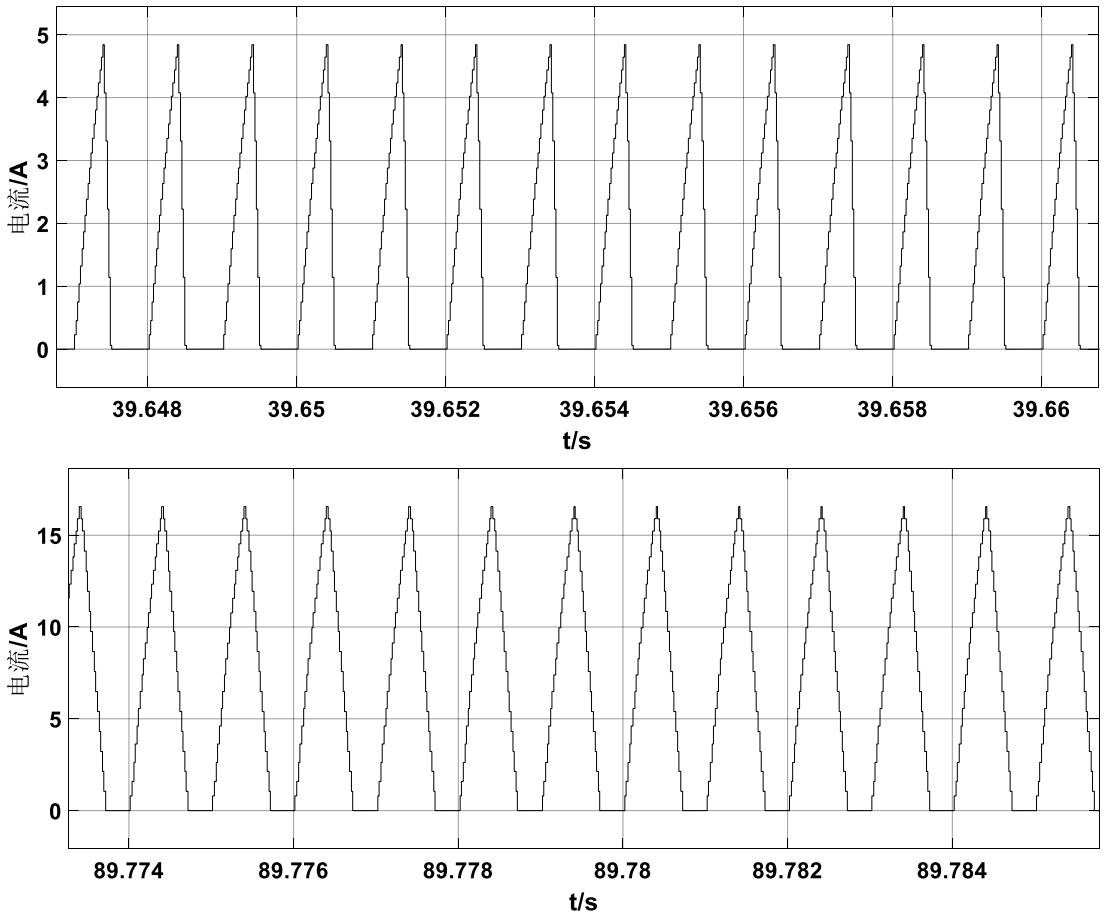

ISSN: 2664-9640

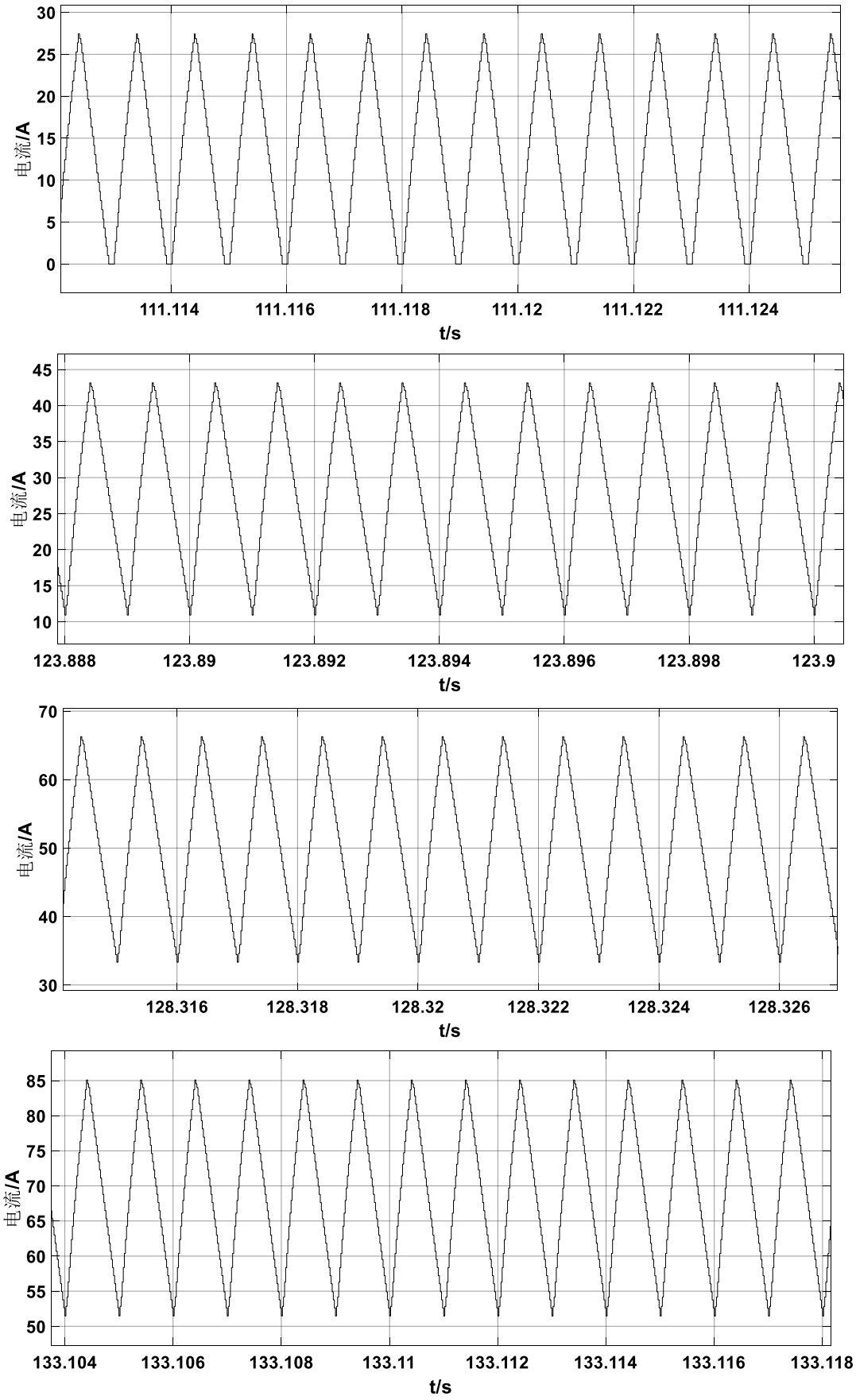

Fig.13 Six steady state inductance current of active balancing circuit

ISSN: 2664-9640

The SOC inconsistency of each battery is optimized after the battery pack balancing. Before the battery pack balances, the range of each battery SOC is 7%. After the accomplishment of the active balancing process, the maximum range between the battery SOC is reduced to 1.2%, and the balancing time is only 133 s.

The balancing method proposed in this work improves the consistency of batteries in the battery pack effectively and the performance of the entire battery pack.

3. Conclusion

A novel active balancing circuit has been designed to solve the inconsistency problem of lithium-ion batteries in the battery packs of new energy vehicles. EKF algorithm has been used to transform the measured battery voltage to battery SOC accurately. Afterwards, an active balancing circuit has been designed and used to the battery pack, which manifests excellent performance in balancing experiment. The next step of the research is applied the balancing circuit to electric vehicles in the actual test.

Acknowledgments

This work was supported by the National Natural Science Foundation of China under Grant No. 51607004, Collaborative Innovation Project of Anhui Universities, No.GXXT-2019-002, Natural Science Research Key Project of Education Department of Anhui Province No.KJ2018A0369 and College Students Innovation and Entrepreneurship Training Program of Anhui Province No.S202010372125X.

References

[1] Amine K , Belharouak I , Chen Z , et al. Organic Nonvolatile Memory: Nanostructured Anode Material for High-Power Battery System in Electric Vehicles (Adv. Mater. 28/2010)[J]. Advanced Materials, 2010, 22(28):0-0.

[2] Yao H E , Liu X T , Zhang C B , et al. Insulation detection algorithm for high-power battery system based on internal resistance model[J]. Journal of Jilin University, 2013.

[3] Finkelstein A , Gabbay D M , Hunter A , et al. Inconsistency Handling in Multiperspective Specifications[J]. IEEE Transactions on Software Engineering, 2002, 20(8):569-578.

[4] Thaler R H . Some Empirical Evidence on Dynamic Inconsistency[J]. Economics Letters, 1981, 8(3):201-207.

[5] Finkelstein A , Gabbay D M , Hunter A , et al. Inconsistency Handling in Multiperspective Specifications[J]. IEEE Transactions on Software Engineering, 2002, 20(8):569-578.

[6] Wang, W. Q . A self-balancing circuit to measure capacitance and loss conductance for industrial transducer. [J]. IEEE Transactions on Instrumentation & Measurement, 1996.

[7] Li S , Mi C , Zhang M . A High Efficiency Active Battery Balancing Circuit Using Multi-Winding Transformer[J]. IEEE Transactions on Industry Applications, 2013, 49(1):198-207.

[8] Ye Y , Cheng K . An Automatic Switched-Capacitor Cell Balancing Circuit for Series-Connected Battery Strings[J]. Energies, 2016, 9(3):138.

[9] Carpenter R O . A New Light Balancing Circuit for the Non-Recording Densitometer*[J]. Journal of the Optical Society of America (1917-1983), 1946, 36(11):676-678.

[10] Liu L , Li G . Battery cell monitoring and balancing circuit: US, US20040257042 A1[P]. 2004.

[11] Phillips J R , Daniel L , Silveira L M . Guaranteed Passive Balancing Transformations for Model Order Reduction[J]. IEEE Transactions on Computer-Aided Design of Integrated Circuits and Systems, 2002, 22(8):1027-1041.

ISSN: 2664-9640

[12] Phillips J , Daniel L , Silveira L M . Guaranteed passive balancing transformations for model order reduction[C]// Proceedings 2002 Design Automation Conference (IEEE Cat. No.02CH37324). IEEE, 2002.

[13] Taplak H , Erkaya S , Uzmay. Passive balancing of a rotating mechanical system using genetic algorithm[J]. Scientia Iranica, 2012, 19(6):1502-1510.

[14] Moon J D , Kim B S , Lee S H . Development of the active balancing device for high-speed spindle system using influence coefficients[J]. International Journal of Machine Tools & Manufacture, 2006, 46(9):978-987.

[15] Park J , Haan J , Park F C . Convex Optimization Algorithms for Active Balancing of Humanoid Robots[J]. IEEE Transactions on Robotics, 2007, 23(4):817-822.

[16] F Baronti, Roncella R , Saletti R . Performance comparison of active balancing techniques for lithium-ion batteries[J]. Journal of Power Sources, 2014, 267:603-609.

[17] Pou J , Pindado R , D Boroyevich. Voltage-balance limits in four-level diode-clamped converters with passive front ends[J]. IEEE Transactions on Industrial Electronics, 2005, 52(1):190-196.

[18] Pou J , Pindado R , D Boroyevich. Voltage-balance limits in four-level diode-clamped converters with passive front ends[C]// Conference of the IEEE Industrial Electronics Society. IEEE, 2002.

[19] Jalali A A , Mohammadi F , Ashrafizadeh S N . Effects of process conditions on cell voltage, current efficiency and voltage balance of a chlor-alkali membrane cell[J]. Desalination, 2009, 237(1-3):126-139.

[20] Piller S , Perrin M , Jossen A . Methods for state-of-charge determination and their applications[J]. Journal of Power Sources, 2001, 96(1):113-120.

[21] Aylor J H , Thieme A , Johnso B W . A battery state-of-charge indicator for electric wheelchairs[J]. IEEE Transactions on Industrial Electronics, 1992, 39(5):398-409.

[22] He Z , Zhong C , Xun H , et al. Simultaneous enhancement of open-circuit voltage, short-circuit current density, and fill factor in polymer solar cells.[J]. Advanced Materials, 2011, 23(40):4636-4643.

[23] V, D, Mihailetchi, et al. Cathode dependence of the open-circuit voltage of polymer:fullerene bulk heterojunction solar cells[J]. Journal of Applied Physics, 2003, 94(10):6849-6849.

[24] Bolognani S , Oboe R , Zigliotto M . Sensorless full-digital PMSM Drive with EKF estimation of speed and rotor position[J]. IEEE Trans Industrial Electronics, 1999, 46(1):184-191.

[25] Yim E , Darling E M , Kulangara K , et al. Nanotopography-induced changes in focal adhesions, cytoskeletal organization, and mechanical properties of human mesenchymal stem cells.[J]. Biomaterials, 2010, 31(6):1299-1306.